



# Three-dimensional macroporous anodes based on stainless steel fiber felt for high-performance microbial fuel cells



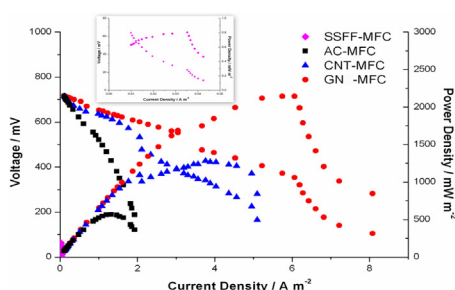
Junxian Hou, Zhongliang Liu\*, Siqi Yang, Yu Zhou

Key Laboratory of Enhanced Heat Transfer and Energy Conservation, Ministry of Education and Key Laboratory of Heat Transfer and Energy Conversion, Beijing Education Commission, College of Environmental and Energy Engineering, Beijing University of Technology, Beijing 100124, PR China

## HIGHLIGHTS

- A novel anode is fabricated based on stainless steel fiber felt.
- The modified SSFFs as anodes greatly decrease MFCs' internal resistance.
- Metallic backbones combined with carbon nanoparticles are promising for anode design.

## GRAPHICAL ABSTRACT



## ARTICLE INFO

### Article history:

Received 24 November 2013

Received in revised form

20 January 2014

Accepted 9 February 2014

Available online 18 February 2014

### Keywords:

Microbial fuel cell

Macroporous anodes

Graphene

Stainless steel fiber felt

## ABSTRACT

The three-dimensional (3D) macroporous anodes were constructed by coating carbon nanoparticles (graphene, carbon nanotube, or activated carbon) on stainless steel fiber felts (SSFFs) that have an open, solid and macroporous structure. These modified electrodes provided large surface area for reaction, interfacial transport and biocompatible interface available for bacterial colonization and substrate transport. Graphene modified anode delivered a maximum power density of  $2142 \text{ mW m}^{-2}$  at a current density of  $6.1 \text{ A m}^{-2}$  in MFC, greatly improved the performance of MFC compared with the unmodified SSFF-MFC. Electrochemical impedance spectroscopy (EIS) measurements together with the polarization curves demonstrated that carbon nanoparticles modified anodes could greatly decrease MFCs' internal resistance. Our experimental results also proved that embedding carbon nanoparticles into 3D macroporous metallic scaffold is a promising method for MFC anode fabrication.

© 2014 Elsevier B.V. All rights reserved.

## 1. Introduction

Microbial fuel cells (MFCs) can generate electrical power directly utilizing the metabolism of microorganisms, and are a promising approach for simultaneous wastewater treatment and energy recovery [1]. However, the relatively low power density of MFCs remains one of the main obstacles for their practical applications. The

\* Corresponding author.

E-mail addresses: [liuzhl@bjut.edu.cn](mailto:liuzhl@bjut.edu.cn), [liuzl@bjut.edu.cn](mailto:liuzl@bjut.edu.cn), [liuzhl2007@yahoo.com](mailto:liuzhl2007@yahoo.com) (Z. Liu).

total energy loss in the MFC system can be understood from the voltage equation,  $V = E_t - \eta_{\text{ohmic}} - \eta_{\text{act}} - \eta_{\text{conc}}$ , in which  $\eta_{\text{act}}$ ,  $\eta_{\text{ohmic}}$  and  $\eta_{\text{conc}}$  are voltage losses due to ohmic polarization, reaction kinetics and mass transport, respectively [2]. The poor kinetics of the electron transfer between the bacterial cells and anode coupled with diffusion limitation significantly limits power capability of MFCs. Activated loss of electrode is mainly due to the limited reactive area and high activation energy barrier, and the diffusion limitation of electrode stems from the flat structure and relatively smaller micropores of the electrodes. Research have showed that activated loss and diffusion resistance accounting for more than

70% of the total resistance of MFCs [3,4]. An effective way for removing these difficulties is to employ porous electrodes. Porous materials can provide large surface area for reaction, interfacial transport, and dispersion of active sites at different length scales of pores and shorten diffusion paths or reduce diffusion resistance effect [5].

For the MFC anode, macropore that is larger than 50 nm is usually of better performance than micropore (<2 nm) and mesopore (2–50 nm), this is because that the bacterial size is about 1–2  $\mu\text{m}$ . Carbon-based materials are the most common anode materials used in MFCs as they are of good biocompatibility, such as carbon paper, carbon cloth (CC), flat graphite and so on. However, considering practical and large-scale applications, their disadvantages are fatal, such as low strength, high cost, low conductivity and no macropores. Without the macropores, the biofilm can only grow on their surface and is inaccessible to the interior of the anode, and thus the majority of the interior structure is wasted [6]. This limits the anode efficiency seriously. So an open, robust three-dimensional (3D) macroporous structure is desirable because it enables bacterial internal colonization and efficient substrates transport, thus enhance the electron transfer process [7].

To improve the MFC performance, various carbon nanoparticles such as graphene [8,9], carbon nanotube [10], activated carbon [11] had been used to modify the MFC electrodes to minimize the anode energy loss in the system and have significantly increased the MFC power density output. Within this context, embedding nanoparticles into structurally macroporous scaffold as anode is of special relevance for the realistic development of MFC applications, because the resulted materials would offer large contact area between the electrolyte and the electrode and hence increase the specific surface area and reduce the electrode polarization. Xie and his coworkers prepared graphene-based sponges by the simple impregnation of the 3D architectures with graphene sheets. Lab-scale MFCs equipped with these 3D anodes achieved higher volumetric power densities and lower energy losses than the traditional graphite-based anodes. Their study showed that microbial biofilms wrapped the sponge branches, but did not clog the macroscale pores [8].

AISI 316L stainless steel is a common industrial material that has high mechanical properties and long-term resistance to corrosion, and is commercially available in many different compositions and morphologies [12]. The benefits of using stainless steel are many, such as high conductivity, low cost, high strength and the ease of incorporating a flow field [13]. Pocaznoi et al. compared the abilities of carbon cloth, graphite plate and stainless steel to form microbial anodes and demonstrated that stainless steel is a promising electrode material for MFC anode [12]. Herein, we introduce the macroporous AISI 316L stainless steel fiber felt (SSFF) (Fig. S1(a)) made from stainless steel fibers (5–8  $\mu\text{m}$  in diameter). The stainless steel fiber felt has a solid 3D macroporous structure. It remains the most of the excellent properties of stainless steel like high conductivity, strong mechanical strength and high corrosion resistance. Furthermore, as it is shown in Fig. S1(b), its softness is comparable with chemical fibers that is easy to curl and suitable for engineering application.

With these considerations, in this paper, a novel macroporous MFC anode is manufactured from a three-dimensional stainless steel fiber felt (SSFF) that is decorated with the conductive carbon nanoparticles (activated carbon, carbon nanotube, or graphene) by a simple impregnation approach. The SSFF can not only serve as a macroporous and highly conductive scaffold, but also provide the large surface for nanoparticle attachment. The carbon nanoparticles on the scaffold improve the biocompatibility of the stainless steel electrode surface and provide high specific surface area for bacterial attachment. The macroporosity also guarantees

bacterial internal colonization that could enhance electrode reaction. Therefore, carbon nanoparticles modified stainless steel fiber felt is worthy of further investigation with a view to fabricating microbial anodes.

## 2. The experimental

### 2.1. Chemicals and materials

Stainless steel fiber felt (1 mm thick) was purchased from Xi'an Filter Metal Materials Co., Ltd, its mean pore size is 15.7  $\mu\text{m}$  and the porosity is  $78 \pm 5\%$ . Carboxyl graphene and activated carbon were provided by Nanjing XFNANO Materials Tech Co., Ltd. Multi-walled carbon nanotubes (10–20 nm in diameter, 5–15  $\mu\text{m}$  in length) were produced by Shenzhen Nanotech Port Co., Ltd. All chemicals used were of analytical grade and purchased from Beijing Chemical Works. De-ionized water was used in all experiments.

### 2.2. Electrode fabrication

The stainless steel fiber felt (SSFF) substrates were cut into 1.8 cm  $\times$  1.8 cm pieces, and were soaked in acetone for 3 h to dissolve the organic substances adsorbed and then rinsed with the ultrapure water before the experiments. Multi-walled carbon nanotubes were treated using a 3:1 mixture of concentrated  $\text{H}_2\text{SO}_4/\text{HNO}_3$  prior to the experiments and then rinsed with the ultrapure water until its pH value equals to 7, and finally dried at 60  $^\circ\text{C}$ .

To coat the SSFF with carboxyl graphene (GN), the carboxyl graphene was first dispersed in Nafion solution (5 wt.%, DuPont, USA) and de-ionized water by ultrasonic treatment. 4.5  $\mu\text{L}$  of Nafion solution and 0.5 mL of de-ionized water were used for every 1 mg carboxyl graphene. Then the SSFF was immersed into the graphene dispersion for 12 h, allowing the ink to enter the macroscale pores and coat the graphene on the surface and the inner fibers of the SSFF. The indicator for judging the successful attachment of the graphene is its color change from silver-grey to black. After that it was allowed to dry at 60  $^\circ\text{C}$  to finish the fabrication of the graphene modified electrode (GN/SSFF). Activated carbon (AC) and carbon nanotube (CNT) modified stainless steel fiber felts were prepared in the same way, then the AC/SSFF and the CNT/SSFF electrodes were obtained. The final loading of the carbon nanoparticles was  $8 \pm 0.5$  mg.

### 2.3. MFC setup and operation

An H-shaped two-chamber MFC was constructed (6 cm deep, 15  $\text{cm}^2$  of the cross sectional area) for these experiments. The two compartments were separated by a cation exchange membrane (Ultex, Membranes International, Inc., USA), and the volume of each compartment was 90 mL. MFC reactors were inoculated with a mixed bacterial culture from the anode compartment of another H-shaped MFC, which was originally inoculated with domestic wastewater from Beijing Gaobeidian Wastewater Treatment Plant and was operated for more than half a year utilizing acetate.

The cell voltage across the external resistance ( $R_{\text{ext}} = 1000 \Omega$ ) was recorded every 30 min using a data acquisition system (Agilent, USA). Four different anodes (SSFF, AC/SSFF, CNT/SSFF and GN/SSFF) were assembled in the same four reactors and ran in parallel, namely SSFF-MFC, GN-MFC, CNT-MFC and AC-MFC. Carbon felts (1 cm  $\times$  2 cm, Bejing Sanye Co., Ltd, China) were chosen as the cathodes of these MFCs. The anolyte consisted of 1 g  $\text{L}^{-1}$   $\text{CH}_3\text{COONa}$ , 0.3 g  $\text{L}^{-1}$   $\text{NH}_4\text{Cl}$ , 1 g  $\text{L}^{-1}$   $\text{NaCl}$ , 0.04 g  $\text{L}^{-1}$   $\text{CaCl}_2 \cdot 2\text{H}_2\text{O}$ , 0.3 g  $\text{L}^{-1}$   $\text{MgSO}_4$ , 0.2 g  $\text{L}^{-1}$   $\text{NaHCO}_3$ , 10.7 g  $\text{L}^{-1}$   $\text{K}_2\text{HPO}_4$  and 5.3 g  $\text{L}^{-1}$   $\text{KH}_2\text{PO}_4$ . The cathodic compartments of all MFCs were filled with 50 mM ferricyanide and 100 mM phosphate buffer solution

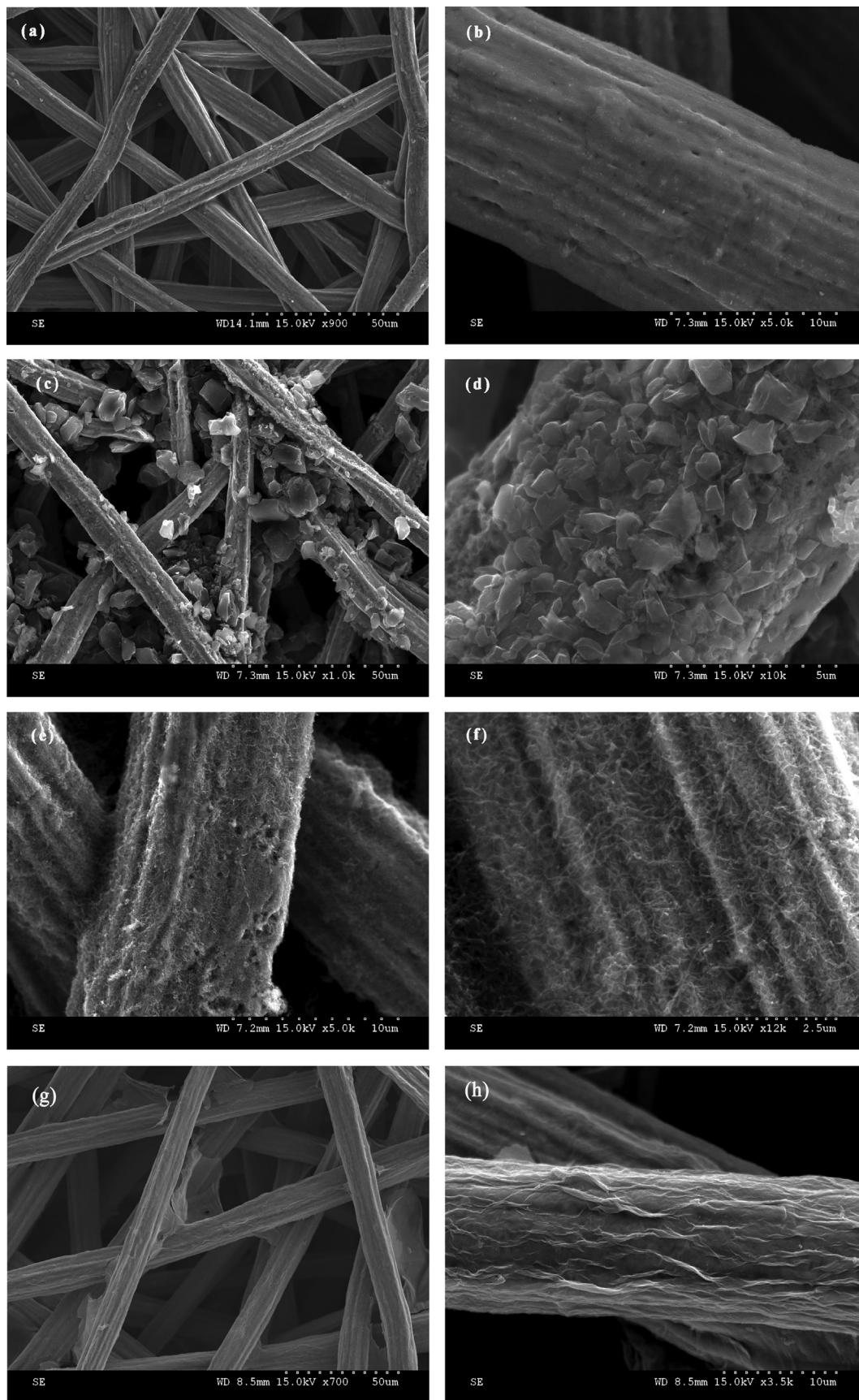


**Fig. 1.** SEM images of the macroporous SSFF and the carbon nanoparticles modified SSFFs. (a) (b) SSFF, (c) (d) SSFF coated with activated carbon, (e) (f) SSFF coated with carbon nanotube, and (g) (h) SSFF coated with carboxyl graphene.

(10.7 g L<sup>-1</sup> K<sub>2</sub>HPO<sub>4</sub>, 5.3 g L<sup>-1</sup> KH<sub>2</sub>PO<sub>4</sub>, pH = 6.9) [10]. The MFCs were operated under the fed-batch mode condition and the anolyte was replaced after the voltage below 50 mV. After 6 weeks operation, power density curves and polarization curves were obtained by changing the circuit external resistor from 9999  $\Omega$  to 50  $\Omega$ . All experiments were carried out in a 33  $\pm$  0.5  $^{\circ}$ C incubator with a 1000  $\Omega$  external resistance connected unless otherwise specified. The power density was normalized based on the projected anodic surface area.

#### 2.4. Characterization

Electrochemical impedance spectroscopy (EIS) was employed to measure the total internal resistances of the MFCs, and the measurements were conducted using the CHI660D (CH Instruments, Shanghai) at the working potential while the MFCs were operated with a constant external resistance ( $R_{\text{ext}} = 1000 \Omega$ ). Two electrode experiments were performed on the whole cell with the anode as the working electrode and the cathode used as the counter and reference electrode in a frequency of 100 kHz to 1 MHz with an AC signal amplitude of 10 mV [4,14,15]. The cyclic voltammograms (CVs) were performed using the CHI660D with a scan rate of 5 mV s<sup>-1</sup> in the three-electrode mode. The anode electrode, the cathode electrode and the Ag/AgCl were used as the working electrode, the counter electrode and the reference electrode, respectively. SEM (Hitachi S-4300N) was employed to characterize the surface morphology of the samples. All experiments were repeated twice and got the similar results.

### 3. Results and discussion

#### 3.1. Morphology analysis

The SEM images in Fig. 1(a) and (b) reveal that the stainless steel fiber felt is a macroporous 3D scaffold with an average pore size of 15.7  $\mu\text{m}$ . This structure is an ideal substrate for fabrication of 3D electrodes used for the MFCs due to its open, solid and highly conductive porous structure that can not only facilitate electrolyte transport but also offer a continuous 3D highly conductive surface for nanoparticles coating. The drawback of the SSFF is that the biocompatibility is not as good as carbon-base anode resulting in limitation of bacterial colonization on the surface of fibers. To solve this problem, carbon nanoparticles were used to modify the SSFF aiming at improving the biocompatibility and decreasing its overpotential as well as increasing the specific surface area accessible for the bacteria colonization. As shown in Fig. 1(d), (f) and (h), compared with the unmodified SSFF Fig. 1(b), the graphene, carbon nanotube and activated carbon modified SSFFs make the fiber surfaces become rough and micro-structuralized. Fig. 1(h) displays SSFF coated with carboxyl graphene, as one can see from this figure, it has a thin wrinkled and crumpled structure. These changes have increased the biocompatibility and the specific surface area that could enhance the interaction between the biofilm and electrode. Moreover, as illustrated in Fig. 1(c), (e) and (g), the conductive coating accords with the felt morphology without changing its open porous structure, so the macropore of the resulting electrode could allow bacteria colonization in the inner structure of the 3D electrode, and thus increase anode reactive surface area.

#### 3.2. Power curve

To investigate the full-cell performance of the carbon nanoparticles modified electrodes, four MFC reactors (SSFF-MFC, AC-MFC, CNT-MFC and GN-MFC) were run in parallel with the same inoculum but different modified anodes for three months.

As shown in Fig. 2, MFCs with the GN/SSFF, CNT/SSFF, AC/SSFF as the anodes reached a stable maximum voltage of 650  $\pm$  10 mV, 620  $\pm$  8 mV, and 580  $\pm$  10 mV, respectively, after 2–3 days operation. These values are about 25 times larger than that of the unmodified SSFF-MFC whose maximum voltage is only 25  $\pm$  4 mV. Actually, it seems that unmodified SSFF-MFC simply did not work. The reasons are many, but the following are among of the most important. As we have pointed out above, the stainless steel is less efficient for interfacial electron transfer, thus it requires a large overpotential [12]. Pocaznoi's experimental results showed that although the microbial anodes formed on stainless steel gave a higher current than those formed on flat graphite, but the stainless steel was revealed to be not able to ensure electron transfer that was as fast as that of graphite or carbon cloth. Furthermore, the stainless steel's biocompatibility is not as good as that of the carbon-based electrodes. Thus, the number of bacteria growing on the fibers is limited and the reactive area of SSFF is small. All these will result in a low electron transfer rate. The carbon nanoparticles modified electrodes offered a desirable integration of the low overpotential, the biocompatible surface and the high reactivity, and these desirable characteristics make the charge transfer at the interface become easier. The micro and mesoporosity of the carbon nanoparticles provides the large reactive surface area and the macroporosity of the SSFF guarantees the bacteria accessible to the inner fibers' surface. The combination of the carbon nanoparticles and the SSFF produces the good performance of the MFC. The graphene modification exhibited a more beneficial effect on the MFC performance than carbon nanotube and activated carbon. It is most likely due to graphene's superior properties, such as its large specific surface area and thin wrinkled and crumpled structure.

The polarization curves and power density curves are illustrated in Fig. 3. From this figure, one can see that the power generation of the GN-MFC, the CNT-MFC and the AC-MFC is much greater than that of the SSFF-MFC. To be specific, the maximum power density of the GN-MFC is 2142 mW m<sup>-2</sup> at a current density of 6.1 A m<sup>-2</sup> and a cell voltage of 373 mV, while the CNT-MFC achieves its maximum power density of 1280 mW m<sup>-2</sup> at the current density of 3.76 A m<sup>-2</sup>, and the maximum power density of the AC-MFC is 560 mW m<sup>-2</sup> at the current density of 1.47 A m<sup>-2</sup>. However, the

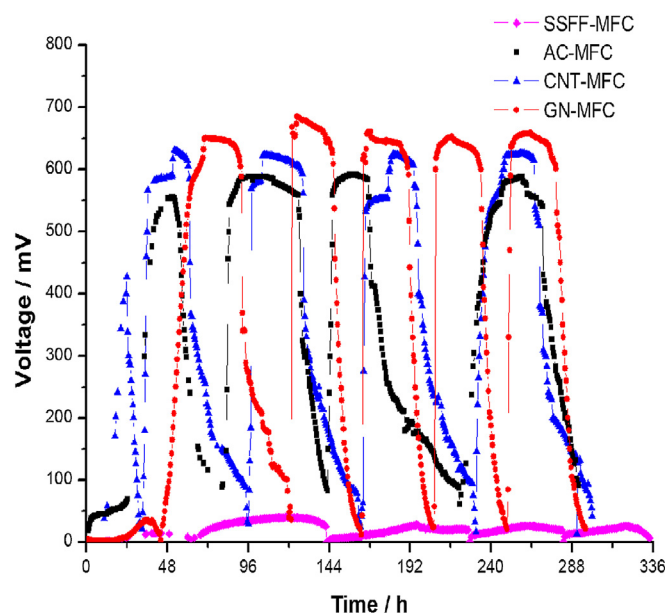


Fig. 2. Voltage output of the SSFF-, AC-, CNT-, and GN-MFC after inoculation.

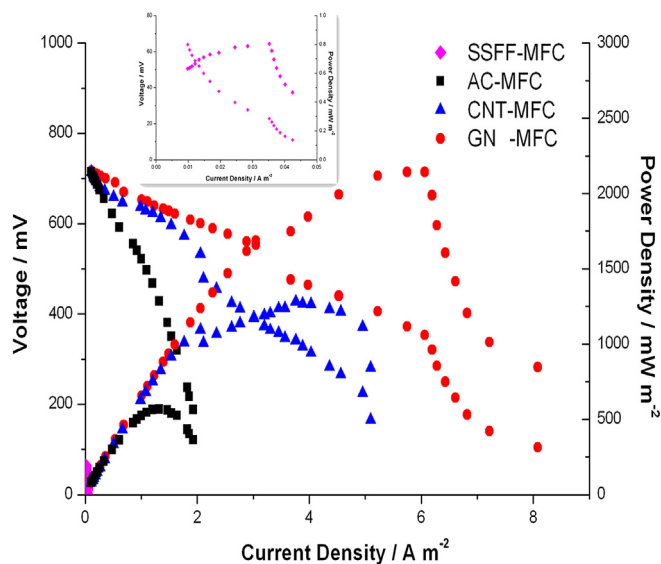


Fig. 3. Polarization curves of the four types of MFCs. The inset is the enlarged polarization curves of the SSFF-MFC.

maximum power density of SSFF-MFC is only  $0.8 \text{ mW m}^{-2}$  at the current density of  $0.035 \text{ A m}^{-2}$ . This may be due to the high overpotential and the poor biocompatibility of the SSFF, as we have pointed out above. Another two MFCs were assembled employing carbon cloth (CC,  $1.8 \text{ cm} \times 1.8 \text{ cm}$ ) and graphene modified CC (GN/CC,  $1.8 \text{ cm} \times 1.8 \text{ cm}$ ) as anode respectively. The polarization curves were shown in Fig. S2, the unmodified CC-MFC obtained a maximum power density of  $476 \text{ mW m}^{-2}$  at the current density of  $1.11 \text{ A m}^{-2}$ , better than the SSFF-MFC. In summary, stainless steel fiber felt could not be directly used as anode. But after the modification, the power density of the GN-MFC is  $2142 \text{ mW m}^{-2}$ , significantly higher than that of the GN/CC-MFC which is only  $1014 \text{ mW m}^{-2}$  (Fig. S2). Therefore, the use of durable metallic backbones combined with a thin layer of carbon nanoparticles could offer exciting opportunities in the advancement of MFC anode design. The total internal resistance ( $R_{\text{int}}$ ) of an MFC can be obtained from the slope of the linear part of the polarization curves, as suggested by Yan et al. [14]. The calculated total internal resistance of the SSFF-MFC is  $983 \Omega$ , while the total internal resistance of the GN-MFC, the CNT-MFC and the AC-MFC is only  $89 \Omega$ ,  $141 \Omega$  and  $345 \Omega$ , respectively. It proves that the carbon nanoparticles modified stainless steel fiber felt could greatly reduce the total internal resistance of MFCs due to the increased anode reactive specific area and electron transfer rate.

### 3.3. Electrochemical analysis

The larger reactive specific surface area and higher electron transfer efficiency of the carbon nanoparticles modified anodes enable the higher output power density of the MFCs than the unmodified SSFF anode. To verify this, the electrochemical performance of the four type anodes is tested in parallel in the MFCs after 6 weeks operation. Cyclic voltammograms are recorded at the maximum of the bioelectrocatalytic activity after replenishment of the medium. As showed in Fig. 4, the *in situ* voltammograms of the carbon nanoparticles modified anodes show larger current than that of the unmodified SSFF, indicating an enhanced electron transfer rate due to the optimized structure of the anodes, especially of the graphene modified electrode which benefits from the graphene's property. The CV curves of the four anodes all show two

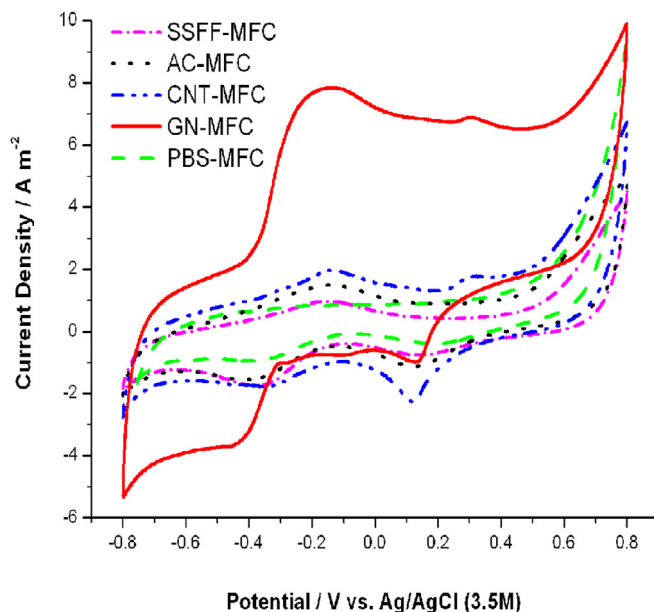


Fig. 4. The cyclic voltammograms of the unmodified SSFF and carbon nanoparticles modified SSFFs as anodes in the MFCs at the scan rate of  $5 \text{ mV s}^{-1}$ .

couples of the redox peaks. The right pairs were believed to originate from the electrochemical activity of the stainless steel itself because it is also observed in the PBS-MFC that using the unmodified SSFF as the anode and the anolyte only contains the phosphate buffer solution without bacteria (Fig. 4). So they should not be related to the electron transfer from the bacteria because the midpoint potential of these redox peaks is greater than  $0 \text{ V}$  and much higher than the reaction potential of our MFC anodes which is significantly smaller than  $0 \text{ V}$  [15]. The left pairs of CV curves in Fig. 4 are identified as biofilm redox characteristic. A peak current of  $7.83 \text{ A m}^{-2}$  at  $-0.16 \text{ V}$  in the oxidation scan and a peak current of  $-3.69 \text{ A m}^{-2}$  at  $-0.45 \text{ V}$  in the reduction scan are clearly observed at the GN-SSFF. Compared with the GN-SSFF, the other three electrodes (the SSFF, the AC-SSFF and the CNT-SSFF) exhibit comparatively smaller redox peaks. This may be contributed to the

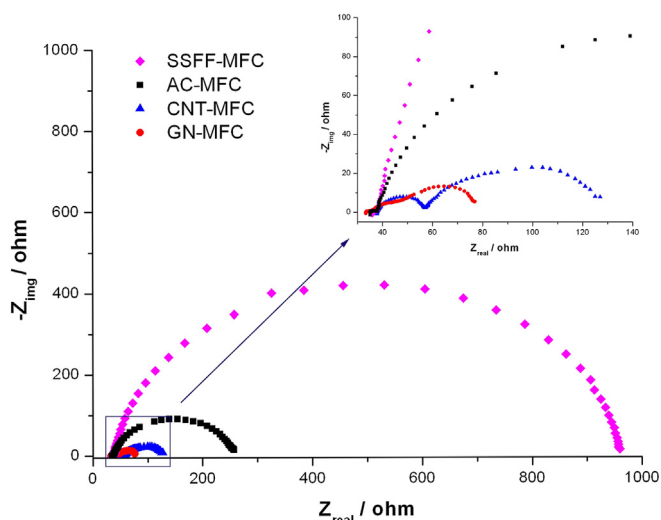


Fig. 5. EISs of the SSFF-, AC-, CNT-, and GN-MFC under working cell conditions using two-electrode mode. The inset is the enlarged EIS curves.

increased biofilm loading and the enhanced electron transfer efficiency resulted from the excellent properties of the graphene.

To understand the influence of the carbon nanoparticles modified anodes on the total resistance of the MFCs better, two-electrode mode EIS experiments are conducted for all the MFCs under working cell condition ( $R_{\text{ext}} = 1000 \Omega$ ). After the steady-state current generation achieved, and the Nyquist plots are obtained and shown in Fig. 5. Impedance studies of MFCs' whole resistance with different anodes often use a two time-constant model for resistance estimation [3,4,16]. In our experiments, inductive behavior was observed at high-frequency for all the SSFF based MFCs, but it did not appear in carbon cloth based MFCs [9]. This maybe attribute to metallic components and the porosity of the electrodes [17–19]. So the equivalent circuit  $LR_1(R_2Q)(R_3C)$  is used here, calculate the MFCs' total resistance, in which  $L$  represents the inductance,  $R_1$  represents the ohmic resistance, and  $R_2$  the charge transfer resistance,  $R_3$  and  $C$  in parallel represent the finite diffusion [3,4,16]. By fitting the data of the Nyquist plots, the estimated total resistance of the GN-MFC, the CNT-MFC and the AC-MFC is 84.2  $\Omega$ , 136.7  $\Omega$ , and 285.8  $\Omega$ , respectively, which are all much smaller than that of the SSFF-MFC whose total resistance is calculated to be 974.5  $\Omega$ . The measured solution resistance  $R_s$  of the four MFCs is about 33  $\Omega$ . Therefore, the polarization resistance of the SSFF-MFC is 941.5  $\Omega$ , while that of the GN-MFC, the CNT-MFC and the AC-MFC is 51.2  $\Omega$ , 103.7  $\Omega$  and 252.8  $\Omega$ , respectively. The EIS results demonstrate that carbon nanoparticles modified anodes can greatly decrease the polarization resistance and have good electrochemical kinetics and of course can produce a higher power output. It also confirms that embedding carbon nanoparticles into macroporous metallic scaffold is a promising and effective method for anode fabrication. It should also be noted that the total resistance obtained from the EIS measurements is in accordance with the estimation result of the whole cell resistance using the linear part of the polarization curves as stated in Section 3.2, which confirms the reliability of the present experimental results to some extent.

#### 4. Conclusion

A novel 3D macroporous electrode was fabricated by coating the carbon nanoparticles on 3D stainless steel fiber felts. The experimental results showed that these modified electrodes as anodes greatly improved the performance of MFCs. The reason is that the carbon nanoparticles modified electrodes offer a desirable integration of the low overpotential, the biocompatible surface and the high reactivity, which makes the charge transfer at the interface easier. GN-MFC gave a much higher power output than the CNT-MFC and the AC-MFC, likely because graphene's superior properties greatly enhanced its electron transfer efficiency. The results of

the EIS measured resistance is in good agreement with the estimations using the linear part of the polarization curves, which demonstrates that carbon nanoparticles modified SSFF can greatly decrease the polarization resistance and shows good electrochemical kinetics. This study also proves that the carbon nanoparticles modification of the 3D macroporous metallic scaffold is a promising and effective method for the fabrication of high-performance anodes. However, metal-based materials used as the MFC anode have a risk of corrosion, so further research is required and the long-term operation is needed to confirm its practical application effectiveness.

#### Acknowledgments

This work is supported by the Chinese National Natural Science Foundation Project (No. 51076004).

#### Appendix A. Supplementary data

Supplementary data related to this article can be found at <http://dx.doi.org/10.1016/j.jpowsour.2014.02.035>.

#### References

- [1] B.E. Logan, K. Rabaey, *Science* 337 (2012) 686–690.
- [2] P.Y. Zhang, Z.L. Liu, *J. Power Sources* 195 (2010) 8013–8018.
- [3] A.J. Hutchinson, J.C. Tokash, B.E. Logan, *J. Power Sources* 196 (2011) 9213–9219.
- [4] Y. Ahn, B.E. Logan, *Energy Fuels* 27 (2013) 271–276.
- [5] Y. Li, Z.Y. Fu, B.L. Su, *Adv. Funct. Mater.* 22 (2012) 4634–4667.
- [6] R. Thorne, H.N. Hu, K. Schneider, P. Bombelli, A. Fisher, L.M. Peter, A. Dent, P.J. Cameron, *J. Mater. Chem.* 21 (2011) 18055–18060.
- [7] X. Xie, M. Ye, L.B. Hu, N. Liu, J.R. McDonough, W. Chen, H.N. Alshareef, C.S. Criddle, Y. Cui, *Energy Environ. Sci.* 5 (2012) 5265–5270.
- [8] X. Xie, G.H. Yu, N. Liu, Z.N. Bao, C.S. Criddle, Y. Cui, *Energy Environ. Sci.* 5 (2012) 6862–6866.
- [9] J.X. Hou, Z.L. Liu, P.Y. Zhang, *J. Power Sources* 224 (2013) 139–144.
- [10] J.E. Mink, J.P. Rojas, B.E. Logan, M.M. Hussain, *Nano. Lett.* 12 (2012) 791–795.
- [11] F. Zhao, N. Rahunen, J.R. Varcoe, A. Chandra, C.A. Rossa, A.E. Thumser, R.C.T. Slade, *Environ. Sci. Technol.* 42 (2008) 4971–4976.
- [12] D. Pocanai, A. Calmet, L. Etcheverry, B. Erable, A. Bergel, *Energy Environ. Sci.* 5 (2012) 9645.
- [13] N. Heras, E.P.L. Roberts, R. Langton, D.R. Hodgson, *Energy Environ. Sci.* 2 (2009) 206–214.
- [14] Y.Z. Fan, E. Sharbrough, H. Liu, *Environ. Sci. Technol.* 42 (2008) 8101–8107.
- [15] Y.C. Yong, X.C. Dong, B.C. Park, H. Song, P. Chen, *ACS Nano* 6 (2012) 2394–2400.
- [16] Y. Yin, G.T. Huang, Y.R. Tong, Y.D. Liu, L.H. Zhang, *J. Power Sources* 237 (2013) 58–63.
- [17] L.H.J. Raijmakers, D.L. Danilov, J.P.M. van Lammeren, M.J.G. Lammers, P.H.L. Notten, *J. Power Sources* 247 (2014) 539–544.
- [18] E.E. Ferg, F. van Vuuren, *Electrochim. Acta* (2013). <http://dx.doi.org/10.1016/j.electacta.2013.08.110>.
- [19] W.J. Gao, S. Cao, Y.Z. Yang, H. Wang, J. Li, Y.M. Jiang, *Thin Solid Films* 520 (2012) 6916–6921.